

Structural evolution and property changes in $\text{Nd}_{60}\text{Al}_{10}\text{Fe}_{20}\text{Co}_{10}$ bulk metallic glass during crystallization

Zhi Zhang, Lei Xia, and Ru Ju Wang

Institute of Physics, Chinese Academy of Sciences, Beijing 100080, People's Republic of China

Bing Chen Wei

National Microgravity Laboratory, Institute of Mechanics, Chinese Academy of Sciences, Beijing 100080, People's Republic of China

Ming Xiang Pan and Wei Hua Wang^{a)}

Institute of Physics, Chinese Academy of Sciences, Beijing 100080, People's Republic of China

(Received 12 July 2002; accepted 5 October 2002)

The structural evolution and property changes in $\text{Nd}_{60}\text{Al}_{10}\text{Fe}_{20}\text{Co}_{10}$ bulk metallic glass (BMG) upon crystallization are investigated by the ultrasonic method, x-ray diffraction, density measurement, and differential scanning calorimetry. The elastic constants and Debye temperature of the BMG are obtained as a function of annealing temperature. Anomalous changes in ultrasonic velocities, elastic constants, and density are observed between 600–750 K, corresponding to the formation of metastable phases as an intermediate product in the crystallization process. The changes in acoustic velocities, elastic constants, density, and Debye temperature of the BMG relative to its fully crystallized state are much smaller, compared with those of other known BMGs, the differences being attributed to the microstructural feature of the BMG. © 2002 American Institute of Physics. [DOI: 10.1063/1.1525053]

Recently, many glass forming alloys were discovered.^{1,2} Previous studies show that the crystallization in various bulk metallic glasses (BMGs) is characterized by the appearance of intermediate metastable phases. The formation of icosahedral phases as an intermediate product of the crystallization process in BMGs indicates that there is a structural relationship between the BMGs and quasicrystalline.^{3,4} The Nd-based BMGs have also evoked intensive interests due to their unique magnetic properties and anomalous crystallization behavior.^{1,5–7} It is found that the microstructural change induced by relaxation and crystallization has a very sensitive effect on the thermal and magnetic properties of the BMGs. This implies that the hard magnetic property of the BMGs may be related to the formed intermediate phases prior to the crystallization. In this letter, the microstructural and property changes in the $\text{Nd}_{60}\text{Al}_{10}\text{Fe}_{20}\text{Co}_{10}$ BMG upon crystallization are investigated by using ultrasonic method and density measurement, which are effective and sensitive tools for studying the structural and vibrational characteristics of BMGs.^{8–11} The structural and property features, prior to and in the crystallization process, are connected.

$\text{Nd}_{60}\text{Al}_{10}\text{Fe}_{20}\text{Co}_{10}$ BMG was prepared by the die casting method.⁶ The BMG rod was cut to a length of about 10 mm and its ends were polished flat and parallel. Afterward, the sample was stepwise isothermally annealed at various temperatures for 1.0 h in a vacuum of 10^{-3} Pa, respectively. After each annealing, the rod was cooled to room temperature, and the acoustic velocities and density were measured. The acoustic velocities were measured by a pulse echo overlap method using a MATEC 6600 ultrasonic system with a

10 MHz frequency.^{8,9} The density was measured by the Archimedeon technique and the accuracy is 0.1%. Elastic constants (e.g., Young's modulus E , shear modulus G , bulk modulus K , and Poisson's ratio σ) and Debye temperature Θ_D of the BMG were derived from the acoustic velocities and densities.¹² The structure of the samples was characterized by x-ray diffraction (XRD) using a MAC M03 diffractometer with $\text{Cu } K\alpha$ radiation. Differential scanning calorimeter (DSC) measurements were carried out in a Perkin Elmer DSC-7. The high-resolution transmission electron microscope (HRTEM) performed on a JEOL-2010.

The DSC curves of the $\text{Nd}_{60}\text{Al}_{10}\text{Fe}_{20}\text{Co}_{10}$ BMG at various annealing temperatures (T) are shown in Fig. 1. For the as-cast BMG, the DSC curve shows two exothermal peaks and an endothermic peak. The broad peak with onset temperature (T_{x1}) at 610 K ranges from 610 to 776 K, and the onset temperature T_{x2} of the sharp peak is at 776 K. The broad exothermal phenomenon is common for rare earth (RE)-Fe-Al alloys (RE=Nd, Pr, Y, and Sm) but with alternative and even contradictory explanations for different researchers.^{1,7,13,14} Previous work^{6,7} shows that the magnetic properties of the BMG have been correlated to the intermediate metastable phase that already exists in the as-prepared samples. The hard magnetic properties remain almost unchanged in the annealing-temperature range from room temperature up to 740 K, and disappear after full crystallization of the BMG above 760 K.⁶ The results indicate that the broad exotherm in the DSC curve corresponds to the precipitation of the metastable phase, and the sharp exothermal peak near 776 K is related to the transformation of the metastable to stable crystalline phases and the crystallization of the remaining amorphous phase. When $T < 593$ K, T_{x1} does not show a significant change. When $T > 633$ K, T_{x1} shifts to

^{a)} Author to whom correspondence should be addressed; electronic mail: whw@aphy.iphy.ac.cn

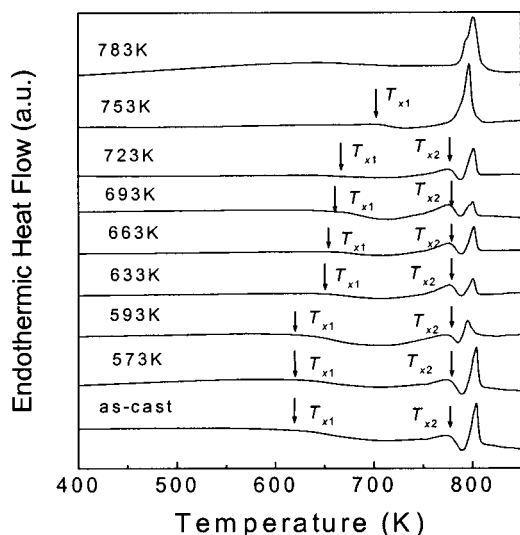


FIG. 1. DSC curves of a series of annealed $\text{Nd}_{60}\text{Al}_{10}\text{Fe}_{20}\text{Co}_{10}$ BMG (at a heating rate of 20 K/min).

a higher temperature with increasing T , and completely disappears at 783 K, while T_{x2} keeps almost unchanged with increasing temperature. The XRD patterns of the BMG in various annealing temperatures are shown in Fig. 2. For $T < 593$ K, XRD patterns confirm that no crystallization occurs. At 633 K, the pattern shows the appearance of equilibrium and metastable phases as marked in Fig. 2. After the sample is successive annealed at higher temperatures, such as 663, 723, and 753 K, other metastable and equilibrium phases are formed as indicated in Fig. 2. The temperature range for the metastable phase precipitation corresponds to that of the broad exothermal peak in a DSC trace. The formation of the metastable phase may be due to favorable kinetics and pre-existing short-range order. At 783 K ($> T_{x2}$), all the metastable phases transform into stable crystalline phases as shown in Fig. 2. The sharp exothermal peak near 776 K in the DSC curve is related to the transformation of the metastable to stable crystalline phases and the crystal-

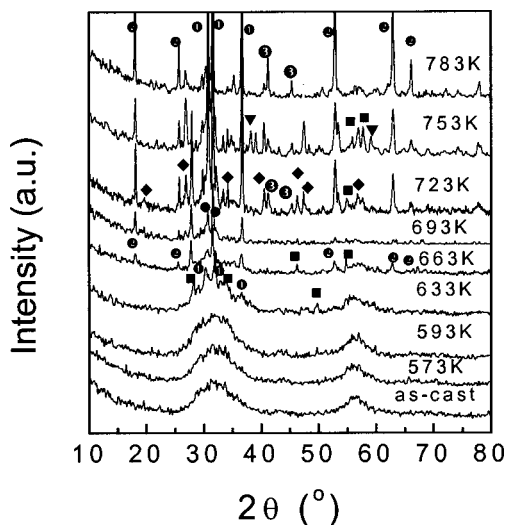


FIG. 2. XRD patterns of a series of annealed $\text{Nd}_{60}\text{Al}_{10}\text{Fe}_{20}\text{Co}_{10}$ BMGs. The sequent appearance of equilibrium phases with increasing temperature are marked by symbols ①, ② and ③, for the metastable phase by ■, ◆, and ▼ indicating that gradual crystallization of BMG and formation of metastable phases with increasing temperature.

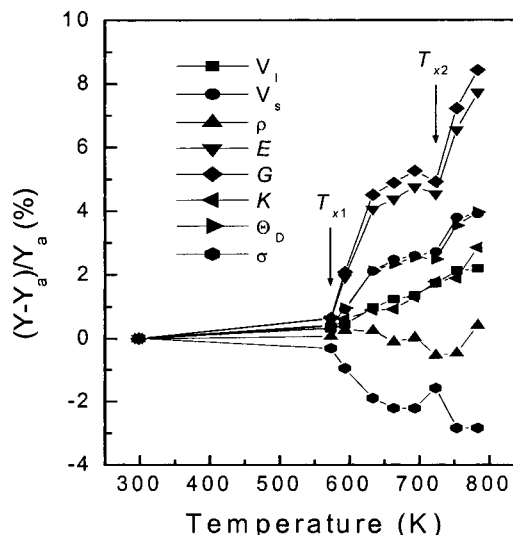


FIG. 3. The relative changes $\Delta Y/Y_a = (Y - Y_a)/Y_a$ of variation of V_l , V_s , ρ , E , G , K , σ , and Θ_D with annealing temperature for $\text{Nd}_{60}\text{Al}_{10}\text{Fe}_{20}\text{Co}_{10}$ BMG. Y and Y_a stand for the properties of glass state and various annealed states of the BMG, respectively.

lization of the remaining amorphous phase. Above 783 K, the BMG is fully crystallized. The some diffraction peaks of the crystallized BMG can be well identified by hexagonal Nd, and a phase corresponds to a paramagnetic $\text{Nd}(\text{Fe}, \text{Co}, \text{Al})_2$ with a MgCu_2 -type structure, respectively.⁷

The values of the ρ , longitudinal velocity, V_l , transverse velocity, V_s of the BMG at ambient condition were 7.047 g/cm^3 , 3.207 km/s, and 1.661 km/s, respectively. The E , G , K , σ , and θ_D calculated from the acoustic data are 51.1 GPa, 19.3 GPa, 46.2 GPa, 0.353, and 188.8 K, respectively. The σ characterizes the relative value of the compressive and shear deformation of a solid. The value of σ of the BMG is close to that of metals, e.g., Cu (0.37)¹⁵ and crystalline alloys, e.g. Monel (0.33),¹⁵ indicating that the BMG has a good plastic deformation. The K/G of the BMG (2.39) is similar to that of metals, such as Cu and steel ($K/G \approx 2.5$). The results indicate that metallic bond is retained even though the BMG lacks long-range order. In fact, the BMG does have some isotropic metallic properties.²

The relative changes of V_l , V_s , and ρ as well as the calculated elastic constants E , G , K , σ , and Θ_D for the BMG as a function of T are presented in Fig. 3. All of the properties exhibit dramatic changes at 575 K. In addition, one anomalous change is observed for the acoustic velocities and elastic constants near 723 K. The ρ increases with temperature below 600 K, but exhibits obvious decreases between 600–750 K. The temperature-dependent properties are ascribed to the progressive ordering as the BMG stepwise undergoes structural relaxation, nanocrystals growth, metastable phase formation and crystallization. It is worth noting that E and G , V_l and K , and V_s and Θ_D exhibit a similar temperature-dependent relationship and almost the same relative variation, respectively, which is in an agreement with other reports.^{10,11} Combining the DSC and XRD results, the dramatic changes at 575 K roughly correspond to the start of the precipitation of the metastable phases in the BMG, the formed metastable phases with lower density lead to the anomalous changes of density between 600–750 K; the

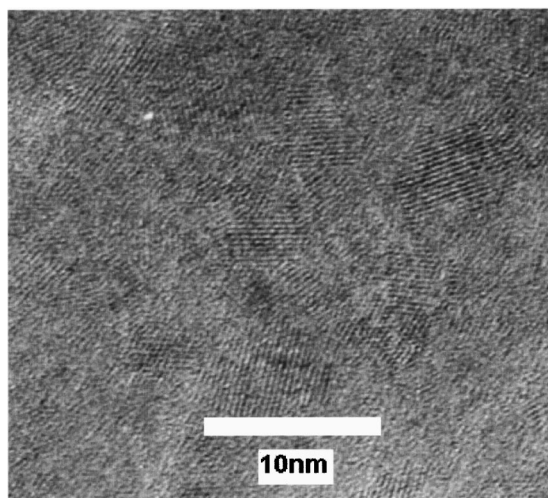
TABLE I. A comparison of the properties of the glassy state (Y_a) and crystallized state (Y_c) for $\text{Nd}_{60}\text{Al}_{10}\text{Fe}_{20}\text{Co}_{10}$, $\text{Pd}_{40}\text{Cu}_{30}\text{Ni}_{10}\text{P}_{20}$ and $\text{Zr}_{41}\text{Ti}_{14}\text{Cu}_{12.5}\text{Ni}_{10}\text{Be}_{22.5}$ alloys.

State	Sample	ρ (g/cm ³)	V_l (km/s)	V_s (km/s)	K (GPa)	G (GPa)	E (GPa)	Θ_D (K)
Glassy state	$\text{Zr}_{41}\text{Ti}_{14}\text{Cu}_{12.5}\text{Ni}_{10}\text{Be}_{22.5}^a$	6.125	5.174	2.472	114.1	37.41	101.2	326.8
	$\text{Pd}_{39}\text{Ni}_{10}\text{Cu}_{30}\text{P}_{21}^b$	9.152	4.750	1.963	159.4	35.3	98.5	279.6
	$\text{Nd}_{60}\text{Al}_{10}\text{Fe}_{20}\text{Co}_{10}$	7.047	3.207	1.661	46.2	19.3	51.1	188.8
Crystallized state	$\text{Zr}_{41}\text{Ti}_{14}\text{Cu}_{12.5}\text{Ni}_{10}\text{Be}_{22.5}^a$	6.192	5.446	2.807	118.6	48.8	128.7	370.9
	$\text{Pd}_{39}\text{Ni}_{10}\text{Cu}_{30}\text{P}_{21}^b$	9.209	4.902	2.208	161.4	44.9	123.3	314.0
	$\text{Nd}_{60}\text{Al}_{10}\text{Fe}_{20}\text{Co}_{10}$	7.076	3.277	1.726	47.4	20.9	55.1	196.0
$(Y_c - Y_a)/Y_a$ (%)	$\text{Zr}_{41}\text{Ti}_{14}\text{Cu}_{12.5}\text{Ni}_{10}\text{Be}_{22.5}^a$	1.1	5.2	13.5	3.9	30.3	27.2	13.4
	$\text{Pd}_{39}\text{Ni}_{10}\text{Cu}_{30}\text{P}_{21}^b$	0.62	3.2	12.5	1.2	27.3	25.1	12.3
	$\text{Nd}_{60}\text{Al}_{10}\text{Fe}_{20}\text{Co}_{10}$	0.41	2.2	3.9	2.6	8.3	7.8	3.8

^aData taken from Ref. 9.^bData taken from Ref. 8.

anomalous changes observed in acoustic velocities and elastic constants around 723 K are attributed to the transformation of the metastable phases. Because the DSC and the annealed specimens for acoustic measurements have a different thermal treatment history, on which the crystallization strongly depends, the temperature variations of elastic constants just roughly correspond to the DSC curve.

The relative changes in acoustic velocity, ρ , elastic constants, $\text{Pd}_{39}\text{Cu}_{30}\text{Ni}_{10}\text{P}_{21}$ and $\text{Zr}_{41}\text{Ti}_{14}\text{Cu}_{12.5}\text{Ni}_{10}\text{Be}_{22.5}$ BMGs Θ_D between glassy and crystallized states of the BMG are summarized in Table I. After crystallization, the value of ρ of the Nd-based BMG increases only $\sim 0.41\%$, and much smaller than those of $\text{Pd}_{39}\text{Cu}_{30}\text{Ni}_{10}\text{P}_{21}$ (0.62%),⁸ $\text{Zr}_{41}\text{Ti}_{14}\text{Cu}_{12.5}\text{Ni}_{10}\text{Be}_{22.5}$ (1.1%)⁹ BMGs and ordinary metallic glasses (1% to 2%).¹⁶ The relative changes in V_s , G , and Θ_D are also much smaller than the corresponding values of Pd-based and Zr-based BMGs. The comparison indicates that the Nd-based BMG shows much smaller softening of the transverse phonon relative to its crystallized state. It is known that the softening of the transverse phonon is a common phenomenon in glasses.¹⁷ The anomalous result can be understood from the microstructure of the BMG. Figure 4 exhibits an HRTEM image of the as-cast $\text{Nd}_{60}\text{Al}_{10}\text{Fe}_{20}\text{Co}_{10}$ BMG. A large numbers of ordered regions (clusters and

FIG. 4. HR TEM image of the as-cast $\text{Nd}_{60}\text{Al}_{10}\text{Fe}_{20}\text{Co}_{10}$ BMG.

nanocrystals) are dispersed in the glassy matrix. The size of these heterogeneous and disoriented ordered regions is smaller than 10 nm, but the volume fraction is as large as 50%. The BMG has more dense packing state and results in the much smaller changes in density, acoustic properties, and smaller transverse phonon softening.

In conclusion, anomalous changes in ultrasonic velocities, elastic constants, and density are observed in the $\text{Nd}_{60}\text{Al}_{10}\text{Fe}_{20}\text{Co}_{10}$ BMG during crystallization, which correspond to the formation of metastable phases as an intermediate product. The changes in acoustic velocities, elastic constants, density, and Θ_D relative to full crystallization are much smaller compared with that of other known BMGs, which are attributed to the mixture microstructure of nanocluster and glass.

The authors are grateful for the financial support of National Natural Science Foundation of China (Grant N.S. 59925101, 50031010, and 10174088).

¹A. Inoue, *Acta Mater.* **48**, 279 (2000).²W. L. Johnson, *MRS Bull.* **24**, 42 (1999).³U. Köster, J. Meinhardt, S. Roos, and R. Busch, *Mater. Sci. Eng., A* **226**, 955 (1997).⁴M. W. Chen, T. Zhang, A. Inoue, and T. Sakurai, *Appl. Phys. Lett.* **75**, 1697 (1999).⁵Y. He, C. E. Price, and S. J. Poon, *Philos. Mag. Lett.* **70**, 371 (1994).⁶B. C. Wei, W. H. Wang, M. X. Pan, and W. R. Hu, *Phys. Rev. B* **64**, 012406 (2000).⁷L. Q. Xing, J. Eckert, W. Loser, S. Roth, and L. Schultz, *J. Appl. Phys.* **88**, 3565 (2000).⁸L. M. Wang, W. H. Wang, R. J. Wang, Z. J. Zang, D. Y. Dai, and L. L. Sun, *Appl. Phys. Lett.* **77**, 1147 (2000).⁹W. H. Wang, L. L. Li, M. X. Pan, and R. J. Wang, *Phys. Rev. B* **63**, 052204 (2001).¹⁰N. Nishiyama, A. Inoue, and J. Z. Jiang, *Appl. Phys. Lett.* **78**, 1985 (2001).¹¹W. H. Wang, R. J. Wang, D. Q. Zhao, M. X. Pan, and Y. S. Yao, *Phys. Rev. B* **62**, 11 292 (2000).¹²D. Schreiber, *Elastic Constants and Their Measurement* (McGraw-Hill, New York, 1973).¹³Y. Li, S. C. Ng, Z. P. Lu, Y. P. Peng, and K. Lu, *Philos. Mag. Lett.* **78**, 213 (1998).¹⁴B. C. Wei, Y. Zhang, Y. X. Zhuang, D. Q. Zhao, M. X. Pan, W. H. Wang, and W. R. Hu, *J. Appl. Phys.* **89**, 3529 (2001).¹⁵D. E. Gray, *American Institute of Physics Handbook*, 3rd ed. (McGraw-Hill, New York, 1973), Chap. 3.¹⁶H. S. Chen, *Rep. Prog. Phys.* **43**, 23 (1980).¹⁷N. Q. Lam and P. R. Okamoto, *MRS Bull.* **17**, 41 (1994).